

Altered Mitral Valve Kinematics with Atrioventricular and Ventricular Pacing

Frank Langer¹, Frederick A. Tibayan¹, Filiberto Rodriguez¹, Tomasz Timek¹, Mary K. Zasio¹, David Liang², George T. Daughters³, Neil B. Ingels³, D. Craig Miller¹

¹Department of Cardiovascular and Thoracic Surgery, ²Division of Cardiovascular Medicine, Stanford University School of Medicine, Stanford, California, ³Laboratory of Cardiovascular Physiology and Biophysics, Research Institute of the Palo Alto Medical Foundation, Palo Alto, California, USA

Background and aim of the study: Pacing-induced mitral regurgitation contributes to the 'pacemaker syndrome', which usually is observed with ventricular (V) pacing, but has also been reported with atrioventricular (AV) sequential pacing. Effects of different pacing modes on 3-D kinematics of the mitral apparatus are incompletely understood.

Methods: Radio-opaque markers were placed on the left ventricular (LV) and mitral apparatus including the annulus, leaflets and papillary muscles of eight sheep. Hemodynamic and 3-D dynamic marker geometry were obtained one week later with biplane videofluoroscopy (60 Hz) during atrial (pacing site = left atrium), AV-sequential (140 ms interval) and (anterolateral LV epicardial) ventricular pacing.

Results: Compared with A-pacing (*p <0.05): 1) The regurgitant fraction increased with both AV- and V-pacing (A: 6 ± 3%, AV: 13 ± 3%*, V: 15 ± 2%*); 2) AV and V-pacing delayed closure at the leaflet center (A: 21 ± 10 ms, AV: 52 ± 5 ms*, V: 92 ± 6 ms*) and posterior commissure (A: 17 ± 10 ms, AV: 46 ± 8 ms*, V: 94 ± 6 ms*). V-pacing delayed valve closure at the ante-

rior commissure (A: 27 ± 9 ms, V: 94 ± 6 ms*); 3) The end-diastolic leaflet opening angle was greater with AV- and V-pacing (anterior mitral leaflet (AML): A: 32 ± 2°, AV: 41 ± 4°*, V: 46 ± 4°*; posterior mitral leaflet (PML): A: 56 ± 4°, AV: 62 ± 3°*, V: 68 ± 3°*); 4) 'Effective' end-diastolic PML midline length was reduced with AV- and V-pacing (A: 11.2 ± 0.7 mm, AV: 10.0 ± 0.4 mm*, V: 10.2 ± 0.3 mm*), as was the distance from each papillary muscle (PM) tip to the AML edge ('effective' chordal length) close to the commissures (anterior PM-AML: A: 31.5 ± 1.8 mm, AV: 30.5 ± 1.9 mm*, V: 29.7 ± 1.8 mm*; posterior PM-AML: A: 33.7 ± 1.8 mm, AV: 33.1 ± 1.9 mm*, V: 32.8 ± 1.9 mm*).

Conclusion: Both ventricular and AV-sequential-pacing resulted in a more widely opened valve at end-diastole and leaflet dyssynchrony with delayed mitral valve closure and early systolic mitral regurgitation. These alterations which result in pacing-induced mitral regurgitation may be clinically important in patients with impaired LV function.

The Journal of Heart Valve Disease 2005;14:286-294

The 'pacemaker syndrome' is an iatrogenic disorder with clinical symptoms ranging from fatigability to syncope. This syndrome results from hemodynamic sequelae of ventricular pacing (V-pacing), and occurs in up to 15% of patients (1-6). Asynchronous V-pacing causes mitral regurgitation (MR), which appears to be a contributory factor to the 'pacemaker syndrome'. The resolution of clinical symptoms and echocardiographic evidence of MR usually occurs after changing

to a dual-chamber system with atrioventricular sequential pacing (AV-pacing) (7-9). Based on these findings, AV-sequential pacing is believed to be a more physiologically normal pacing mode (10). Recent studies, however, reported the incidence of MR in patients with dual-chamber devices and AV-sequential pacing (11,12). Loss of presystolic mitral area reduction has been identified as a possible underlying mechanism of MR in V-pacing (10,13), but underlying mechanisms for pacing-induced MR associated with AV-pacing have not yet been characterized.

The aim of the present study was to elucidate the kinematics of mitral valve closure (14) during atrial (A), atrioventricular (AV) and ventricular (V) pacing. Since LV-pacing sites have become increasingly popular with the advent of biventricular pacing and cardiac resynchronization therapy (15-17), the closure dynamics of the entire mitral valve apparatus was examined

Presented at the Second Biennial Meeting of the Society for Heart Valve Disease, 28th June-1st July 2003, Palais des Congrès, Paris, France

Address for correspondence:

D. Craig Miller MD, Department of Cardiothoracic Surgery, Falk Cardiovascular Research Center, Stanford University School of Medicine, Stanford, CA 94305-5247, USA
e-mail: dcm@stanford.edu

during different pacing modes with the anterolateral LV wall as pacing site.

Materials and methods

Surgical preparation

Eight adult male sheep (mean body weight 74 ± 5 kg) were premedicated with ketamine (25 mg/kg, i.m.), and anesthesia was induced with sodium thiopental (6.8 mg/kg, i.v.) and maintained with inhalational isoflurane (1-2.5%). Through a left thoracotomy, nine tantalum myocardial markers (#2-10; Fig. 1A) were inserted in the left ventricular (LV) subepicardium and septum along four equally spaced longitudinal meridians, with one marker at the LV apex (#1). After establishment of cardiopulmonary bypass (CPB), tantalum markers were placed at the tips of both the anterior and posterior papillary muscles (APM #13, #14 and PPM #11, #12), and eight markers were sutured around the circumference of the mitral annulus (one near each commissure (#16, #20) and three along the septal (#15, 21, 22) and lateral (#17, 18, 19) annulus perimeter (Fig. 1B). Leaflet edge markers were sutured to the ventricular side of the anterior mitral leaflet (AML) and posterior mitral leaflet (PML) at the leaflet center (#26, 27; Fig. 1B) and towards the anterior commissure (ACOM) (#29, 30) and posterior commissure (PCOM) (#31, 32). Markers were also sutured along the midlines of the AML (#23, 24, 25; Fig. 1B) and PML (#28). The atriotomy was closed, the heart de-aired, the cross-clamp removed, and the heart defibrillated (mean CPB time 84 ± 8 min; mean aortic cross-clamp time 62 ± 4 min). An implantable micromanometer pressure transducer (PA4.5-X6; Konigsberg Instruments, Inc., Pasadena, CA, USA) was placed in the LV chamber through the apex and exteriorized through the skin between the scapulae. Bipolar epicardial pacing leads were placed at the left atrial auricle and the anterolateral LV wall. The chest was closed and the animal allowed to recover.

Experimental protocol

After a mean acclimatization period of 8 ± 1 days, each animal was taken to the cardiac catheterization laboratory, sedated with ketamine (1-4 mg/kg/h, i.v. infusion) and diazepam (5 mg, i.v.), intubated, mechanically ventilated, and maintained with inhalational isoflurane (1-2.5%). A micromanometer catheter (Millar Instruments, Inc., Houston, TX, USA) was introduced through a sheath in the left carotid artery and advanced to the aortic arch for aortic pressure measurement.

Simultaneous biplane videofluoroscopic marker data and hemodynamic data were acquired during A-pacing, AV-sequential pacing with an AV-interval at

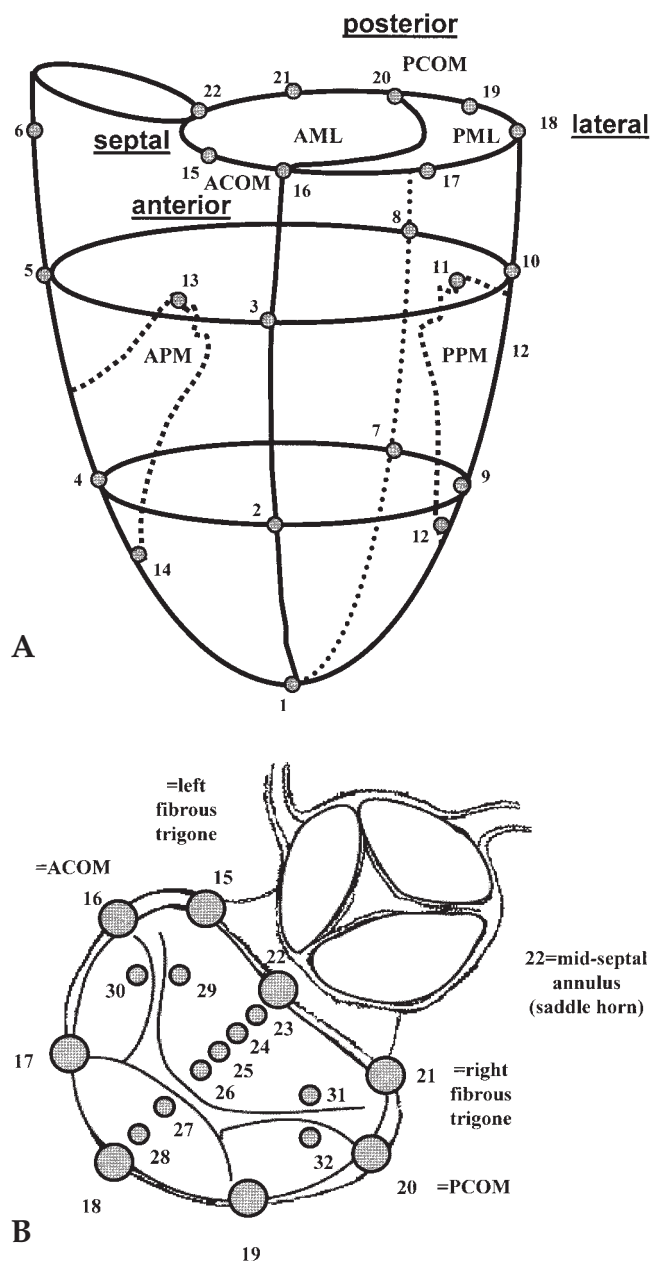


Figure 1: A) Schematic representation of the radio-opaque marker array utilized in this study. B) Schematic representation of the radio-opaque annular and leaflet markers utilized in this study. AML: Anterior mitral leaflet; PML: Posterior mitral leaflet; ACOM: Anterior commissure; PCOM: Posterior commissure; APM: Anterior papillary muscle; PPM: Posterior papillary muscle.

140 ms and asynchronous V-pacing, all at rates of 110-120 per min (Medtronic™ DDD 4653) to override the native sinus rate.

All animals received humane care in compliance with the *Principles of Laboratory Animal Care* formulated by the National Society for Medical Research and the

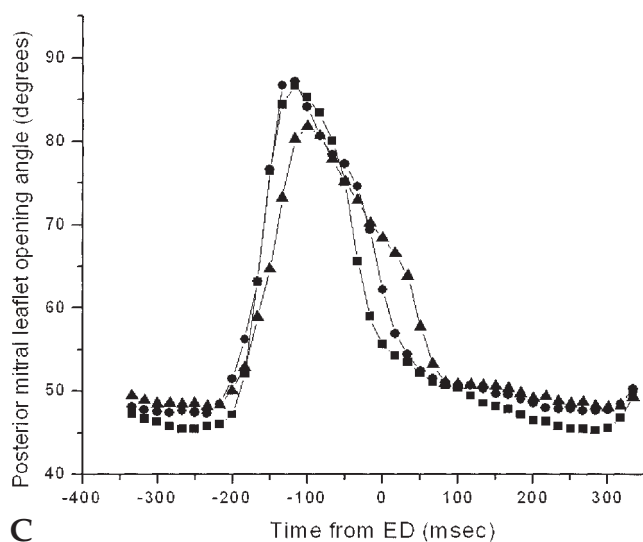
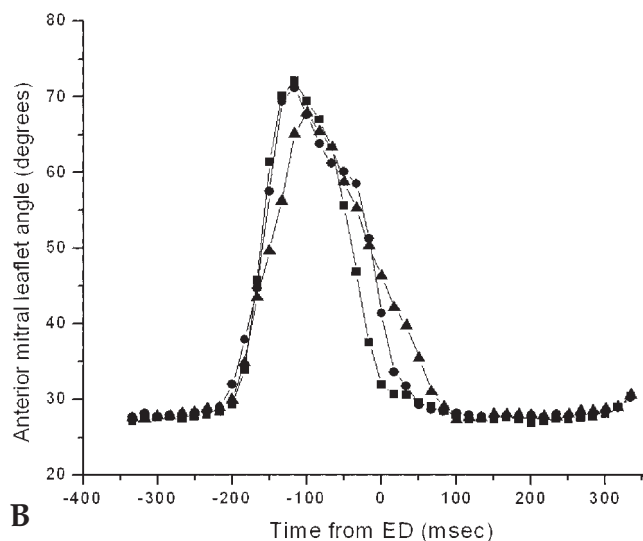
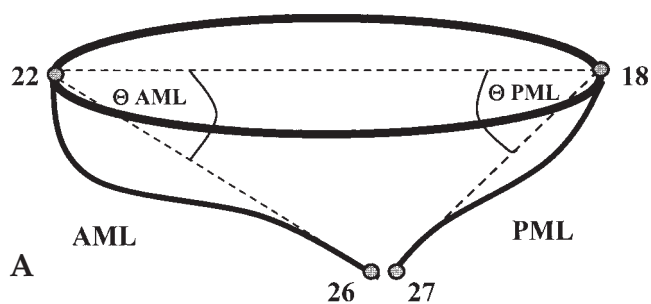


Figure 2: A) Schematic representation of the radio-opaque annular and leaflet markers defining leaflet angle. B) Anterior mitral leaflet angle versus time during A-pacing (■), AV-pacing (●) and V-pacing (▲). C) Posterior mitral leaflet angle versus time during A-pacing (■), AV-pacing (●) and V-pacing (▲). Abbreviations as Figure 1.

Guide for Care and Use of Laboratory Animals prepared by the National Academy of Sciences and published by the National Institutes of Health (DHEW NIHG publication 85-23, revised 1985). This study was approved by the Stanford University Medical School Laboratory Research Animal Review committee and conducted according to Stanford University policy. Correct marker position was verified in all animals post mortem.

Data acquisition

Images were acquired with the animal in the right lateral position with a biplane videofluoroscopy system (Philips Medical Systems, North America Company, Pleasanton, CA, USA). Data from the two radiographic views were digitized and merged to yield 3-D coordinates for each of the radio-opaque markers every 16.7 ms using custom software (18). The accuracy of 3-D-reconstructions from biplane videograms of length measurements, expressed as mean percentage error of a known marker-to-marker 3-D-length, was shown to be 0.2% with a reproducibility of 1% (19). Aortic pressure, LV pressure, and electrocardiogram (ECG) voltage signals were digitized and recorded simultaneously during marker data acquisition.

Data analysis

Cardiac cycle timing and hemodynamics

Two consecutive steady-state beats during each pacing intervention were averaged and defined as A-pacing, AV-pacing and V-pacing data for each animal. For each cardiac cycle, end-systole (ES) was defined as the time of the peak rate of LV pressure (LVP) fall ($-dP/dt$), and end-diastole (ED) at the time of maximum of the second derivative of LVP, corresponding with the frame immediately before the upstroke of the upstroke of the LVP curve as well the peak of the ECG R-wave. Instantaneous LV volume was calculated for each frame (i.e., every 16.7 ms) from the positions of the epicardial LV markers and annular markers using a space-filling multiple tetrahedral volume method (20). Stroke volume (SV) was calculated as end-diastolic volume (EDV) minus end-systolic volume (ESV). Leaflet closure times were defined as the time after ED when each leaflet edge marker pair (ACOM #29-#30, CENTER #26-#27, PCOM #31-#32) achieved minimum separation distance in 3-D space. The regurgitant volume (RV) for each beat was calculated as the difference between EDV and the LV volume at the latest leaflet closure time at leaflet center, ACOM or PCOM. The regurgitant fraction (RF) was calculated as RV/SV .

Leaflet dynamics

Leaflet angles were calculated as the angle between lines through the middle of the septal and lateral mitral annulus (#22-#18; Fig. 2A) and leaflet base and the cen-

Table I: Hemodynamic data.

Parameter	A-pacing	AV-pacing	V-pacing	p-value
Heart rate (bpm)	112.9 ± 1.1	110.7 ± 0.4	114.5 ± 2.2	NS
dP/dt _{max} (mmHg/s)	1,360.0 ± 90.4	1,244.3 ± 87.6	1,319.2 ± 103.3	NS
LVEDV (ml)	160.9 ± 11.5	162.6 ± 11.4	157.0 ± 12.1*	0.003
SV (ml)	35.6 ± 2.9	35.8 ± 2.8	32.9 ± 2.4*	0.007
LVEDP (mmHg)	25.5 ± 2.1	24.0 ± 1.9	20.3 ± 3.6*	0.005
V _{regurg} (ml)	2.1 ± 1.1	5.1 ± 1.3	5.0 ± 1.0	0.06
F _{regurg} (%)	5.5 ± 2.8	13.3 ± 2.6*	14.6 ± 2.2*	0.02

Data expressed as mean ± SEM, RM ANOVA with Dunnett's post-hoc-testing, Friedman's Repeated Measures ANOVA on ranks with Dunnett's post-hoc-testing (LVEDP).

*p <0.05 compared with A-pacing.

LVEDP: Left ventricular end-diastolic pressure; LVEDV: Left ventricular end-diastolic volume; NS: Not significant; SV: Stroke volume.

ter leaflet edge markers respectively (#22-#26 for AML, #18-27 for PML). 'Effective' leaflet midline length was defined as the distance between the leaflet edge markers and their corresponding annular markers (AML: #26-#22; PML: #27-#18; see Fig. 1B). 'Effective' chordal length was measured as distance between each papillary muscle tip and its associated leaflet edge marker (APM: #13-#29 (commissural), #13-#30 (commissural), #13-#26 (central), #13-#27 (central); PPM: #11-#31 (commissural), #11-#32 (commissural), #11-26 (central), #11-#27 (central); Fig. 1A and B).

Mitral annular geometry

Mitral annular area was calculated as the sum of the areas of eight triangles formed by consecutive adjacent marker pairs on the annulus (#15-22; Fig. 1B) and the annular centroid. The septal-lateral (S-L) diameter of the annulus was calculated as the distance in 3-D space between the two markers placed in the middle of the septal and lateral mitral annulus (#22 and 18; Fig. 1B). The annular commissure-commissure (C-C) diameter was calculated as the distance between the two commissural markers (#16 and #20; Fig. 1B).

Papillary muscles

Papillary muscle tip positions were characterized as the distance from each papillary muscle tip to the corresponding commissure (APM-ACOM: #13-#16, PPM-

PCOM: #11-#20; Fig. 1A and B). Papillary muscle length was defined as the distance between each papillary tip and base marker (APM: #13-#14, PPM: #11-#12; Fig. 1A).

Statistical analysis

All data were reported as mean ± SEM. Comparisons between the different pacing modes were made using a Repeated Measures ANOVA after normal distribution had been tested with a Kolmogorov-Smirnov-test. If the data were distributed in a non-Gaussian manner (LVEDP only), Friedman's Repeated Measures ANOVA on Ranks was applied. Dunnett's test was applied for post-hoc testing with A-pacing as control group. A p-value ≤0.05 was considered to be statistically significant (denoted by *).

Results

The mean hemodynamic data during all pacing conditions are summarized in Table I. Heart rate and dP/dt_{max} were similar at all times. Compared with A-pacing, LVEDV, SV and LVEDP decreased with V-pacing. Regurgitant fraction increased with both AV-pacing (13 ± 3%*) and V-pacing (15 ± 2%*) compared with A-pacing (6 ± 3%). Ventricular pacing also increased mitral annular area, S-L diameter, and C-C

Table II: End-diastolic mitral annular dimensions

Dimension	A-pacing	AV-pacing	V-pacing	p-value
S-L diameter (mm)	28.0 ± 1.0	28.0 ± 1.0	29.0 ± 1.0*	0.004
C-C diameter (mm)	38.0 ± 1.6	38.0 ± 1.5	38.7 ± 1.5*	0.001
Mitral annular area (cm ²)	8.47 ± 0.57	8.48 ± 0.58	8.96 ± 0.56*	<0.001

Data expressed as mean ± SEM, RM ANOVA with Dunnett's post-hoc testing.

*p <0.05 compared with A-pacing.

S-L: Septal-lateral; C-C: Intercommissural.

Table III: Leaflet dynamics.

Parameter	A-pacing	AV-pacing	V-pacing	p-value
Valve closure at CENTER (ms)	20.9 ± 10.3	52.2 ± 4.9*	91.9 ± 6.3*	<0.001
Valve closure at ACOM (ms)	27.1 ± 9.4	48.0 ± 8.0*	93.9 ± 6.3*	<0.001
Valve closure at PCOM (ms)	16.7 ± 10.0	45.9 ± 7.6*	93.9 ± 6.3*	<0.001
End-diastolic AML angle (°)	31.9 ± 1.8	41.3 ± 3.8*	46.3 ± 3.8*	0.003
End-diastolic PML angle (°)	55.6 ± 3.9	62.2 ± 3.2*	68.4 ± 3.1*	0.001

Data expressed as mean ± SEM, RM ANOVA with Dunnett's post-hoc-testing.
 *p <0.05 compared with A-pacing.

diameter at ED size relative to A-pacing (Table II), while AV-pacing did not change these annular dimensions.

The valve closure times at leaflet center, ACOM and PCOM sites are listed in Table III. Relative to A-pacing, significantly delayed closure times were observed with both AV-pacing and V-pacing at the leaflet center, as well as at the PCOM. Additionally, V-pacing delayed valve closure at the ACOM. At ED, leaflet opening angles for both AV-sequential and V-pacing were significantly greater compared with A-pacing (Table III). These results are illustrated graphically for the entire cardiac cycle in Figure 2B. The 'effective' end-diastolic PML midline length was smaller during AV-pacing and V-pacing compared to A-pacing (Table IV). The 'effective' end-diastolic AML midline length tended to be smaller with AV-pacing, but these changes did not attain statistical significance.

'Effective' chordal length at ED (Table V) was smaller for chordae between each PM and their insertion at the AML close to the respective commissure (APM-AML #13-#29; PPM-AML #11-#31) during AV-sequential and V-pacing, whilst all chordal lengths except the PPM to AML leaflet center (#11-#26) were smaller during V-pacing. Compared with A-pacing, V-pacing

reduced the end-diastolic PPM-PCOM distance and both APM and PPM lengths (Table VI). AV-pacing did not change any of these distances or lengths at ED.

Discussion

Competent mitral valve closure is a complex 3-D process requiring precise spatially and temporally coordinated interaction of all involved anatomical structures, including the left atrium, mitral annulus, mitral valve leaflets, chordae tendineae, papillary muscles and left ventricle. Understanding early systolic mitral valve regurgitation associated with pacing necessitates careful measurement of the time-varying 3-D positions of all involved anatomic components throughout most of the cardiac cycle.

Asynchronous V-pacing has been reported to cause MR (1,3-6). Occasionally, this contributes to the 'pace-maker-syndrome', which has symptoms ranging from fatigue to syncope (1). Symptomatic patients have benefited from conversion to AV-sequential pacing systems (7-9). Different mechanisms for pacing-induced MR have been suggested, including LV regional wall motion abnormalities (21,22) and regional ischemia (23). Previous investigations in the present authors'

Table IV: 'Effective' end-diastolic leaflet midline length.

Dimension	A-pacing	AV-pacing	V-pacing	p-value
End-diastolic AML midline length #26-#22 (mm)	19.3 ± 1.0	18.7 ± 0.9	19.3 ± 1.2	0.06
End-diastolic PML midline length #27-#18 (mm)	11.2 ± 0.7	10.0 ± 0.4*	10.2 ± 0.3*	0.02

Data expressed as mean ± SEM, RM ANOVA with Dunnett's post-hoc-testing.
 *p <0.05 compared with A-pacing.

Table V: 'Effective' end-diastolic chordal length.

Dimension [†]	A-pacing	AV-pacing	V-pacing	p-value
Chordae APM-AML (cm)				
Commissural (#13-#29)	31.5 ± 1.8	30.5 ± 1.9*	29.7 ± 1.8*	<0.001
Central (#13-#26)	35.0 ± 1.4	33.9 ± 1.5	32.3 ± 1.5*	0.002
Chordae APM-PML (cm)				
Commissural (#13-#30)	32.7 ± 1.7	32.4 ± 1.6	31.3 ± 1.5*	<0.001
Central (#13-#27)	35.6 ± 1.6	35.8 ± 1.6	35.1 ± 1.4*	0.01
Chordae PPM-AML (cm)				
Commissural (#11-#31)	33.7 ± 1.8	33.1 ± 1.8*	32.8 ± 1.9*	0.003
Central (#11-#26)	35.2 ± 1.4	34.9 ± 1.4	34.4 ± 1.2	0.1
Chordae PPM-PML (cm)				
Commissural (#11-#32)	32.1 ± 1.5	31.9 ± 1.5	31.2 ± 1.4*	0.003
Central (#11-#27)	34.2 ± 1.4	34.0 ± 1.2	33.1 ± 1.0*	0.004

Data expressed as mean ± SEM, RM ANOVA with Dunnett's post-hoc-testing.

[†]Commissural = chordae inserting in the leaflet edge close to the commissure; central = chordae inserting in the central leaflet edge.

*p <0.05 compared with A-pacing.

laboratory characterized some underlying mechanisms for MR induced by V-pacing (10,13). In sinus rhythm, the mitral annular area shrinks prior to systole in sheep, suggesting a sphincteric function facilitating mitral valve closure. This presystolic mitral area reduction was abolished with V-pacing, resulting in early systolic 'loitering' of the mitral valve leaflets with delayed closure (13,24), and supporting the theory that atrial contraction plays a key role in competent mitral valve closure (25-27) in conjunction with atrioventricular pressure crossover (28). The absence of a proper atrial contraction influences the atrioventricular pressure gradient as one of the closing mechanisms, which can induce mitral regurgitation in atrial fibrillation (29).

Recently, pacing-induced MR has also been described in AV-sequential pacing (11,12). Sassone et al. (11) even reported a higher incidence of mitral regurgitation during DDD (33%) than during VVI (24%) pacing. Other investigators found a correlation between AV-interval and incidence of MR (12,30). Manipulation of the AV-interval may largely influence hemodynamic conditions (30), and may even induce

diastolic MR (31). These observations are discordant with current clinical opinion favoring AV-sequential pacing as being the most physiologic pacing mode.

The experimental data presented herein support these recent contrariwise reports (11,29,30). Compared with atrial pacing, an increased regurgitant fraction was observed during both V-pacing and AV-sequential pacing. In both situations, the valve was in a more widely opened position at ED compared with A-pacing, as reflected by the larger end-diastolic leaflet angles for the AML and PML. Mitral valve closure time was significantly prolonged for V-pacing and for AV-sequential pacing at the leaflet center and at the PCOM-site. Thus, the regurgitant fraction increases due to the mitral valve being in a relatively more open position at ED and closed by a desynchronized mitral apparatus. This dyssynchrony is a sum of multiple alterations including the annulus, leaflets, chordae and papillary muscles, which results in delayed coaptation. Mitral leaflet edge position in 3-D space is determined by connections to the annulus and papillary muscles (32,33). For example, if the papillary muscle tips and the lateral annulus represent the centers of three

Table VI: End-diastolic papillary muscle position and length.

Dimension	A-pacing	AV-pacing	V-pacing	p-value
Distance APM-ACOM (mm)	38.5 ± 1.4	38.4 ± 1.3	38.4 ± 1.3	NS
Distance PPM-PCOM (mm)	40.0 ± 1.6	39.9 ± 1.6	39.6 ± 1.6*	<0.001
APM length (mm)	26.3 ± 2.7	26.3 ± 2.7	25.9 ± 2.7*	<0.001
PPM length (mm)	19.6 ± 3.9	19.8 ± 3.9	19.2 ± 3.9*	<0.001

Data expressed as mean ± SEM, RM ANOVA with Dunnett's post-hoc-testing.

*p <0.05 compared with A-pacing.

NS: Not significant.

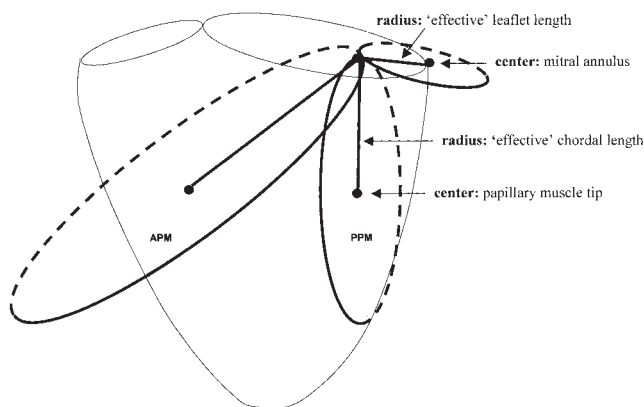


Figure 3: The concept of intersecting spheres. The mitral leaflet edge position in 3-D space is determined by connections to the annulus and papillary muscles. If the papillary muscle tips and the annulus represent the centers of three spheres, and the 'effective' leaflet and chordal lengths represent the radii of these spheres, the position of the leaflet edge will be at a point where the three spheres intersect. The leaflet edge position can be altered by changes in the position of the centers of the spheres (i.e., annulus or PM tip position) or changes of the radii of the spheres (i.e., 'effective' leaflet or chordal lengths).

spheres, and the 'effective' leaflet and chordal lengths represent the radii of these spheres, the position of the PML edge will be at a point where the three spheres intersect (Fig. 3). Leaflet edge position can be altered by changes in the position of the centers of the spheres (i.e., the annulus or PM tip position) or changes in the radii of the spheres (i.e., 'effective' leaflet or chordal lengths). Alterations in annular size (due to loss of presystolic annular contraction during V-pacing) and papillary muscle position are probably due to abnormal activation patterns. A less 'effective' leaflet length implies leaflet furling or rolling, while reduced 'effective' chordal length suggests slack chordae at end-diastole. Altered motion of these involved structures leads to discoordinated interaction which perturbs normal leaflet closure. This desynchronized valve closure may secondarily disturb early systolic LV flow patterns.

Study limitations

One limitation of the present study was the use of an animal model, as certain anatomic differences have been reported between human and sheep cardiac anatomy (34), though ovine cardiac anatomy is generally similar to that in humans (35,36).

Mitral regurgitation was not assessed qualitatively using Doppler echocardiography or ventriculography; however, LV volume changes measured using myocardial marker 3-D LV geometry are extremely precise

and allow quantitative comparisons rather than the subjective qualitative information obtained by other methods. The marker technique with data sampling at 60 Hz allows the acquisition of geometric information at a temporal resolution sufficient to demonstrate timing changes during the isovolumic contraction phase. The spatial resolution of the myocardial marker method provides discrimination of 3-D-coordinates in the sub-millimeter range. It is unlikely that the markers interfered with mitral leaflet motion (aggregate marker mass = 20.6 mg). Even when the AML was grossly overloaded with a large number of heavy markers (total mass 184 mg) in other sheep, the peak AML opening velocity as measured by epicardial pulsed-wave Doppler was similar to that in leaflets without any markers implanted (0.47 ± 0.05 versus 0.45 ± 0.06 m/s). Another limitation of this experiment was the lack of data using different AV-intervals to evoke more pronounced effects (AV-interval = 140 ms). Furthermore, the present experimental model involved animals with normal LV function and conduction system, whereas the deleterious effects of pacing-induced alterations may be even more pronounced in diseased hearts. Finally, only a single ventricular pacing site was used; future studies will need to investigate pacing-induced MR comparing different clinically relevant LV (via epicardial cardiac veins) and RV (via the RV endocardium) pacing sites in order to elucidate the underlying mechanisms.

In conclusion, both V-pacing and AV-sequential pacing from the anterolateral LV epicardium alter mitral valve closure. Based on these observations, atrial pacing is preferable to AV-sequential pacing or ventricular pacing whenever possible. One pertinent clinical example might be after mitral repair, when temporary V- or AV-pacing might lead to erroneous interpretation of valve competence using intraoperative transesophageal echocardiography (37). Since LV pacing sites have become increasingly popular with the advent of cardiac resynchronization therapy (15-17), these results may also be relevant in patients requiring permanent pacing, but this clearly calls for further investigation of the effects of other LV pacing sites on mitral closure kinematics. The adverse effects of LV-based pacing (including more pacing-induced MR) would be especially germane when dealing with patients who have severely impaired LV systolic function and cardiomyopathy, because it is well appreciated that MR begets more MR, thus perpetuating a vicious cycle which is poorly tolerated by patients with advanced heart failure.

Acknowledgements

These studies were funded by grants HL-29589 and

HL-67025 from the National Heart, Lung and Blood Institute. Drs. Langer, Tibayan, Rodriguez and Timek are Carl and Leah McConnell Cardiovascular Surgical Research Fellows. Dr. Langer was supported by the Deutsche Akademie der Naturforscher Leopoldina, Halle, Germany and the Department of Thoracic and Cardiovascular Surgery, University Hospitals Homburg, Homburg/Saar, Germany. Drs. Tibayan and Timek were also supported by NHLBI Individual Research Service Awards HL-10452 and HL-67563. Dr. Rodriguez was supported by Grant HL67025-01S1 from the NHLBI and was an American College of Surgeons Resident Research Scholarship Award. Dr. Timek was also supported by a Research Fellowship Award from the Thoracic Surgery Foundation for Research and Education. The authors appreciate the technical assistance provided by Carol W. Mead, Maggie Brophy, Katha Gazda and Katherine Brooke Harrington.

References

1. Ausubel K, Boal BH, Furman S. Pacemaker syndrome: Definition and evaluation. *Cardiol Clin* 1985;3:587-594
2. Heldman D, Mulvihill D, Nguyen H, et al. True incidence of pacemaker syndrome. *Pacing Clin Electrophysiol* 1990;13(12 Pt.2):1742-1750
3. Berglund H, Nishioka T, Hackner E, et al. Ventricular pacing: A cause of reversible severe mitral regurgitation. *Am Heart J* 1996;131:1035-1037
4. Cannan CR, Higano ST, Holmes DR, Jr. Pacemaker induced mitral regurgitation: An alternative form of pacemaker syndrome. *Pacing Clin Electrophysiol* 1997;20(3 Pt.1):735-738
5. Lee TM, Su SF, Lin YJ, et al. Role of transesophageal echocardiography in the evaluation of patients with clinical pacemaker syndrome. *Am Heart J* 1998;135:634-640
6. Mark JB, Chetham PM. Ventricular pacing can induce hemodynamically significant mitral valve regurgitation. *Anesthesiology* 1991;74:375-377
7. Sulke N, Dritsas A, Bostock J, Wells A, Morris R, Sowton E. 'Subclinical' pacemaker syndrome: A randomised study of symptom free patients with ventricular demand (VVI) pacemakers upgraded to dual chamber devices. *Br Heart J* 1992;67:57-64
8. Hanna SR, Chung ES, Aurigemma GP, Meyer TE. Worsening of mitral regurgitation secondary to ventricular pacing. *J Heart Valve Dis* 2000;9:273-275
9. Kontoyannis SA, Nanas JN, Stamatelopoulos SF. Congestive heart failure treated by the upgrade from VVI to DDD pacing. *Acta Cardiol* 2000;55:41-43
10. Timek T, Dagum P, Lai DT, et al. The role of atrial contraction in mitral valve closure. *J Heart Valve Dis* 2001;10:312-319
11. Sassone B, De Simone N, Parlangei G, Tortorici R, Biancoli S, Di Pasquale G. Pacemaker-induced mitral regurgitation: Prominent role of abnormal ventricular activation sequence versus altered atrioventricular synchrony. *Ital Heart J* 2001;2:441-448
12. Costa M, Elvas L, Ventura M, Cristovao J, Martins R, Providencia L. [Effect of programming different AV intervals on mitral insufficiency in patients with DDD pacemaker]. *Rev Port Cardiol* 2000;19:1285-1288
13. Glasson JR, Komeda M, Daughters GT, et al. Most ovine mitral annular three-dimensional size reduction occurs before ventricular systole and is abolished with ventricular pacing. *Circulation* 1997;96(9 Suppl.):II-22
14. Karlsson MO, Glasson JR, Bolger AF, et al. Mitral valve opening in the ovine heart. *Am J Physiol* 1998;274(2 Pt.2):H552-H563
15. Leclercq C, Kass DA. Retiming the failing heart: Principles and current clinical status of cardiac resynchronization. *J Am Coll Cardiol* 2002;39:194-201
16. Auricchio A, Abraham WT. Cardiac resynchronization therapy: Current state of the art: Cost versus benefit. *Circulation* 2004;109:300-307
17. Willerson JT, Kereiakes DJ. Cardiac resynchronization therapy: Helpful now in selected patients with CHF. *Circulation* 2004;109:308-309
18. Niczyporuk MA, Miller DC. Automatic tracking and digitization of multiple radiopaque myocardial markers. *Comput Biomed Res* 1991;24:129-142
19. Daughters GT, Sanders WJ, Miller DC, Schwartzkopf A, Mead CW, Ingels NB, Jr. A comparison of two analytical systems for three-dimensional reconstruction from biplane videoradiograms. *Proc Comp Cardiol (IEEE)* 1988;15:79-82
20. Moon MR, DeAnda A, Jr., Daughters GT, Ingels NB, Jr., Miller DC. Experimental evaluation of different chordal preservation methods during mitral valve replacement. *Ann Thorac Surg* 1994;58:931-943
21. Maurer G, Torres MA, Corday E, Haendchen RV, Meerbaum S. Two-dimensional echocardiographic contrast assessment of pacing-induced mitral regurgitation: Relation to altered regional left ventricular function. *J Am Coll Cardiol* 1984;3:986-991
22. Prinzen FW, Peschar M. Relation between the pacing induced sequence of activation and left ventricular pump function in animals. *Pacing Clin Electrophysiol* 2002;25(4 Pt.1):484-498
23. Kamp O, de Cock CC, van Eenige MJ, Visser CA. Influence of pacing-induced myocardial ischemia on left atrial regurgitant jet: A transesophageal echocardiographic study. *J Am Coll Cardiol* 1994;23:1584-1591

24. Glasson JR, Komeda M, Daughters GT, et al. Early systolic mitral leaflet 'loitering' during acute ischemic mitral regurgitation. *J Thorac Cardiovasc Surg* 1998;116:193-205
25. Little RC. Effect of atrial systole on ventricular pressure and closure of the A-V valves. *Am J Physiol* 1951;166:289-295
26. Brockman SK. Mechanism of the movement of the atrioventricular valves. *Am J Cardiol* 1963;17:682-690
27. Zacky A, Stenmetz E, Feigenbaum, H. Role of atrium in closure of mitral valve in man. *Am J Physiol* 2003;217:1652-1659
28. Tsakiris AG, Sturm RE, Wood EH. Experimental studies on the mechanisms of closure of cardiac valves with use of roentgen videodensitometry. *Am J Cardiol* 1973;32:136-143
29. Daley R, McMilan IKR, Gorlin R. Mitral incompetence in experimental auricular fibrillation. *Lancet* 2003;269:18-20
30. Rossi R, Muia N, Jr., Turco V, Sgura FA, Molinari R, Modena MG. Short atrioventricular delay reduces the degree of mitral regurgitation in patients with a sequential dual-chamber pacemaker. *Am J Cardiol* 1997;80:901-905
31. Ishikawa T, Sumita S, Kimura K, et al. Critical PQ interval for the appearance of diastolic mitral regurgitation and optimal PQ interval in patients implanted with DDD pacemakers. *Pacing Clin Electrophysiol* 1994;17(11 Pt.2):1989-1994
32. Dagum P, Timek TA, Green GR, et al. Coordinate-free analysis of mitral valve dynamics in normal and ischemic hearts. *Circulation* 2000;102(19 Suppl.3):III62-III69
33. Lai DT, Tibayan FA, Timek TA, et al. Three-dimensional in-vivo dimensions of 'He's triangle' during acute left ventricular ischemia. *J Heart Valve Dis* 2001;10:767-773
34. Walmsley R. Anatomy of human mitral valve in adult cadaver and comparative anatomy of the valve. *Br Heart J* 1978;40:351-366
35. Markovitz LJ, Savage EB, Ratcliffe MB, et al. Large

- animal model of left ventricular aneurysm. *Ann Thorac Surg* 1989;48:838-845
36. Llaneras MR, Nance ML, Streicher JT, et al. Large animal model of ischemic mitral regurgitation. *Ann Thorac Surg* 1994;57:432-439
37. Mihaileanu S, el Asmar B, Acar C, et al. Intra-operative transoesophageal echocardiography after mitral repair - specific conditions and pitfalls. *Eur Heart J* 1991;12(Suppl.B):26-29

Meeting discussion

DR. RADU DEAC (Tirgu-Mures, Romania): I have two questions. First, could you quantitate the level of mitral regurgitation? Second, do you think that this can also happen in a clinical situation?

DR. FRANK LANGER (Stanford, CA, USA): First, we did not use any adjunctive measures such as Doppler echocardiography because the volume measured by the marker method is much more accurate. There were sections of regurgitation with pacing, AV pacing and ventricle pacing, about 14-15% of the stroke volume. You ask if there is any clinical evidence? There are clinical reports of pacing-induced mitral regurgitation in AV-sequential pacing.

DR. DANIEL R. EINSTEIN (Cleveland, OH, USA): I have seen your reports where you looked at posterior mitral annular dilatation and found a delay in the closing of the posterior leaflet causing an early systolic mitral regurgitation. Could you comment with respect to pacing on the relative timing of the closure of the posterior and anterior leaflets? Are they both delayed? You said that the leaflets are more open - is the anterior leaflet open - does it close earlier than the posterior leaflet - or is it the other way around?

DR. LANGER: The difference in the previous study was that we had leaflets or markers at the center. The present study was the first where we looked at the leaflet center and near both commissures. It is actually a very precise measurement of leaflet closure. It's difficult to tell which leaflet will close first - we may well look into that.